

Learning Dynamical Systems from Data: A Simple Cross-Validation Perspective, Part V: Sparse Kernel Flows for 132 Chaotic Dynamical Systems

Lu Yang^{1,4}, Xiuwen Sun⁵, Boumediene Hamzi^{2,3*}, Houman Owhadi², Naiming Xie¹

¹ College of Economics and Management, Nanjing University of Aeronautics and Astronautics, PR China

² Department of Computing and Mathematical Sciences, Caltech, CA, USA

³ Department of Applied Mathematics and Statistics, Johns Hopkins University, Baltimore, MD, USA.

⁴ Department of Mathematics, Imperial College London, United Kingdom

⁵ Zhejiang Zhelixin Credit Investigation Co., Ltd.

Abstract Regressing the vector field of a dynamical system from a finite number of observed states is a natural way to learn surrogate models for such systems. As shown in [26, 14, 36, 15, 39, 28, 48], a simple and interpretable way to learn a dynamical system from data is to interpolate its vector-field with a data-adapted kernel which can be learned by using Kernel Flows [42].

The method of Kernel Flows is a trainable machine learning method that learns the optimal parameters of a kernel based on the premise that a kernel is good if there is no significant loss in accuracy if half of the data is used. The objective function could be a short-term prediction or some other objective (cf. [26] and [37] for other variants of Kernel Flows). However, this method is limited by the choice of the base kernel.

In this paper, we introduce the method of *Sparse Kernel Flows* in order to learn the “best” kernel by starting from a large dictionary of kernels. It is based on sparsifying a kernel that is a linear combination of elemental kernels. We apply this approach to a library of 132 chaotic systems.

Keywords: System approximation; Chaotic dynamical systems; Learning Kernels; Sparse Kernel Flows

1 Introduction

The ubiquity of time series in many domains of science has led to the development of diverse statistical and machine learning forecasting methods [31, 10, 29, 45, 21, 20, 11, 9, 44, 38, 1].

Amongst various learning-based approaches, kernel-based methods hold the potential for considerable advantages in terms of theoretical analysis, numerical implementation, regularization, guaranteed convergence, automatization, and interpretability [12, 40]. Indeed, reproducing kernel Hilbert spaces (RKHS) [13] has provided strong mathematical foundations for analyzing dynamical systems [29, 22, 16, 18, 32, 23, 33, 34, 3, 35, 6, 7, 8, 24] and surrogate modelling (cf. [46] for a survey). Yet, the accuracy of these emulators depends on the kernel, but limited attention has been paid on the problem of selecting a good kernel.

Recently, experiments by Hamzi and Owhadi [42] have shown that kernel flows (KFs, an RKHS technique) can successfully reconstruct the dynamics of prototypical chaotic dynamical systems under both regular and irregular [36] sampling in time. Given a parameterized kernel function,

* Corresponding author (boumediene.hamzi@gmail.com).

KFs utilizes the regression relative error between two interpolants represented by the kernel (one is obtained by all data points and another is obtained by halved data points) as the quantity to minimize. In this sense, it can also be viewed as a variant of the cross-validation method. Later on, several research has extended the regular Kfs. The nonparametric version of kernel flows, based on kernel warping, is used to approximate chaotic dynamical systems in [14]. A KFs version for SDEs is at [15]. A version for systems with missing dynamics is at [28] and for Hamiltonian dynamics is at [48]. Another version based on the Hausdorff distance to learn attractors is at [37]. From the application perspective, it was used in a machine learning context for classification [49] and more recently in geophysical forecasting [25].

It is worth noting that although the aforementioned kernel learning algorithms can obtain optimal parameters of the kernel from data, it requires a base kernel, making it sub-optimal for practitioners to select an appropriate kernel function for a given practical problem. In this work, we introduce the method of *Sparse Kernel Flows* to discover the ‘best’ kernel from time series. It is based on starting with a base kernel that contains a large number of terms and then sparsifying it by setting some of the initial terms to zero. The principal contributions are summarized as follows:

- (1) Given a base kernel that consists of the sum of a relatively large number of elemental kernels, we develop the algorithm of *Sparse Kernel Flows*. The sparsity is obtained via ℓ_1 -regularization. Starting from the initial base kernel, the goal of the method is to seek the “best” kernel with as few terms as possible with the “best” emulation characteristic.
- (2) In order to evaluate the generalization performance and accuracy of our proposed Sparse Kernel Flows algorithm, we apply the proposal to a chaotic dynamical system benchmark including 132 systems.

The remaining parts are organized as follows. Section 2 states the problem and proposes the Sparse Kernel Flows algorithm. Section 3 consists of numerical experiments where we apply the method of Sparse Kernel Flows to the 132 chaotic dynamical systems library in [19] to evaluate the generalization and accuracy. Section 4 concludes the work.

2 Statement of the problem and its proposed method

Given a time series x_1, \dots, x_n from a deterministic dynamical system in \mathbb{R}^d , our goal is to forecast the evolution of the dynamics from historical observations.

A natural solution to forecasting the time series is to assume that the data are sampled from a discrete dynamical system

$$x_{k+1} = f^\dagger(x_k, \dots, x_{k-\tau^\dagger+1}) \quad (1)$$

where $x_k \in \mathbb{R}^d$ is the state of the system at time t_k , f^\dagger represents the unknown vector field and $\tau^\dagger \in \mathbb{N}^*$ represents the delay embedding or delay.

In order to approximate f^\dagger , given $\tau \in \mathbb{N}^*$ (selection strategies of τ are detailed in [27]), the problem of the dynamical system approximation can be recast as a kernel interpolation problem (employed by [43])

$$Y_k = f^\dagger(X_k), \quad k = 1, \dots, N \quad (2)$$

with $\mathbf{X}_k := (\mathbf{x}_{k+\tau-1}, \dots, \mathbf{x}_k)$, $\mathbf{Y}_k := \mathbf{x}_{k+\tau}$ and $N = n - \tau$ for $\tau \in \mathbb{N}^*$.

Given a reproducing kernel Hilbert space¹ of candidates \mathcal{H} for f^\dagger , and using the relative error in the RKHS norm $\|\cdot\|_{\mathcal{H}}$ as a loss, the regression of the data $(\mathbf{X}_k, \mathbf{Y}_k)$ with the kernel $k : \mathbb{R}^n \times \mathbb{R}^n \rightarrow \mathbb{R}$ associated with \mathcal{H} provides a minimax optimal approximation [41] of f^\dagger in \mathcal{H} . This regressor (in the presence of measurement noise of variance $\lambda > 0$) is

$$f(\mathbf{x}) = K(\mathbf{x}, \mathbf{X})(K(\mathbf{X}, \mathbf{X}) + \lambda \mathbf{I})^{-1} \mathbf{Y} \quad (3)$$

where $\mathbf{X} = (\mathbf{X}_1, \dots, \mathbf{X}_N)$, $\mathbf{Y} = (\mathbf{Y}_1, \dots, \mathbf{Y}_N)$, $K(\mathbf{x}, \mathbf{X})$ is the $N \times N$ matrix with entries $k(\mathbf{x}, \mathbf{X}_i)$, $K(\mathbf{X}, \mathbf{X})$ is the $N \times N$ matrix with entries $k(\mathbf{X}_i, \mathbf{X}_j)$, \mathbf{I} is the identity matrix and $\lambda_1 \geq 0$ is a hyper-parameter that ensures the matrix $K(\mathbf{X}, \mathbf{X}) + \lambda \mathbf{I}$ invertible. This regressor has also a natural interpretation in the setting of Gaussian process (GP) regression: (3) is the conditional mean of the centred GP $\xi \sim \mathcal{N}(0, K)$ with covariance function K conditioned on $\xi(\mathbf{X}_k) = \mathbf{Y}_k + \sqrt{\lambda} \mathbf{Z}_k$ where the \mathbf{Z}_k are centered i.i.d. normal random variables.

2.1 A reminder on the Kernel Flows (KF) algorithm

The accuracy of any kernel-based method depends on the kernel k . Here we follow the parametrised KFs algorithm [26] to learn a "good" kernel in the sense that if the number of regression points can be halved without significant loss in accuracy (measured by $\|\cdot\|_{\mathcal{H}}$ associated with the kernel).

To describe this algorithm, let $k_\theta(\mathbf{x}, \mathbf{x}')$ be a family of kernels parameterized by θ , and let $K_\theta(\mathbf{x}, \mathbf{x}')$ be the corresponding gram matrix. The kernel learning iteration procedures of KFs can be described as follows

- (1) Consider a parametrized kernel function k_θ and initialize the parameters θ^0 ;
- (2) Prepare the data vector $\mathbf{X}^b = (\mathbf{X}_1, \dots, \mathbf{X}_N)$ and $\mathbf{Y}^b = (\mathbf{Y}_1, \dots, \mathbf{Y}_N)$ according to the time delay τ ;

Repeat the following until convergence:

- (4) Select $|\mathbf{X}^c| = \lfloor \frac{|\mathbf{X}^b|}{2} \rfloor$ and $|\mathbf{Y}^c| = \lfloor \frac{|\mathbf{Y}^b|}{2} \rfloor$ observations at random among the N observations;
- (5) Design the loss function

$$\rho(\theta) = \frac{\|f^b - f^c\|_{\mathcal{H}}^2}{\|f^b\|_{\mathcal{H}}^2} = 1 - \frac{\mathbf{Y}^{c\top} (K_\theta(\mathbf{X}^c, \mathbf{X}^c) + \lambda \mathbf{I})^{-1} \mathbf{Y}^c}{\mathbf{Y}^{b\top} (K_\theta(\mathbf{X}^b, \mathbf{X}^b) + \lambda \mathbf{I})^{-1} \mathbf{Y}^b} \quad (4)$$

which is the squared relative error (in the RKHS norm $\|\cdot\|_{k_\theta}$ defined by k_θ) between the interpolants f^b and f^c obtained from the two nested subsets of the time series;

- (6) Compute the gradient $\nabla_{\theta} \rho$ with respect of the parameters θ^k ;
- (7) Evolve the parameter in the gradient descent direction of ρ : $\theta^{k+1} \leftarrow \theta^k - \delta \nabla_{\theta} \rho$.

¹A brief overview of RKHSs is given in the Appendix.

From the training procedures, a key observation is that designing an appropriate kernel function is essential for a specific system approximation problem. While this kernel learning method allows to learn the parameters of a kernel, it also allows some nonzero terms to have very small magnitudes, which may lead to loss of accuracy since they could be zero in reality.

2.2 Proposed Sparse Kernel Flows algorithm

In this section we present the Sparse Kernel Flows algorithm that uses the Least absolute shrinkage and selection operator (Lasso) [47] to sparsify the base kernel. Without loss of generality, let us assume that the base kernel can be written as a linear combination of m kernels:

$$k_{\alpha,\theta} = \sum_{i=1}^m \alpha_i^2 k_i(x, x'; \theta) \quad (5)$$

where k_i is a candidate kernel term, $\theta = (\theta_1, \dots, \theta_m)$ is the intrinsic parameter of candidate kernels, and $\alpha = (\alpha_1, \dots, \alpha_m)$ is the set of weight coefficients that determine the degree of which kernels are active.

Then, the sparsity of coefficients α is achieved by incorporating ℓ_1 regularization into the loss function:

$$\rho(\alpha, \theta) = 1 - \frac{\mathbf{Y}^{c,\top} (K_{\alpha,\theta}(\mathbf{X}^c, \mathbf{X}^c) + \lambda_1 \mathbf{I})^{-1} \mathbf{Y}^c}{\mathbf{Y}^{b,\top} (K_{\alpha,\theta}(\mathbf{X}^b, \mathbf{X}^b) + \lambda_1 \mathbf{I})^{-1} \mathbf{Y}^b} + \lambda_2 \|\alpha\|_1 \quad (6)$$

The proposed approach is distinct from that of the Sparse Spectral Kernel Ridge Regression [2] which incorporates sparsity into the feature-map representation/construction of the Kernel Flows algorithm. In this paper we train the objective function by the SGD optimizer [5] implemented in Pytorch. This results in a trade-off between accurate approximation of the systems and reducing the magnitude of the kernel coefficients, where the trade-off is determined by the regularization penalty λ_2 .

To simultaneously obtain the sparse coefficient of base kernels and intrinsic parameter from data, we solve equation (6) by iterating the following two steps: (a) fix α , optimize θ ; then (b), fix θ , optimize α . The procedure is summarized in Algorithm 1.

Algorithm 1: Sparse Kernel Flows

Input: time series (x_1, \dots, x_n) , embedding delay τ , case kernel $k_{\alpha,\theta}$, hyper-paramter λ_1, λ_2

Output: active kernel function

- 1 Split data into $(\mathbf{X}_1, \dots, \mathbf{X}_N)$ and $(\mathbf{Y}_1, \dots, \mathbf{Y}_N)$, where $N = n - \tau$ // prepare data matrix
 - 2 Random initialize parameters α, θ // initial guess of the base kernel
 - /* update estimates by using KF algorithm presented in Section 2.1 */
 - 3 **for** epoch = 1 : m **do**
 - 4 Fix α , update $\theta \leftarrow \arg \min_{\theta} \rho(\theta|\text{Data})$
 - 5 Fix θ , update $\alpha \leftarrow \arg \min_{\alpha} \rho(\alpha|\text{Data})$
 - 6 **end**
-

The implementation of the training procedures described above requires three tuning hyper-parameters, namely, the embedding delay τ , the shrinkage parameter λ_1 , and the sparsity penalty λ_2 . The choice of these parameters impacts the accuracy of the training procedure. Here we outline some methods for the hyper-parameter selection.

The shrinkage parameter λ_1 avoids overfitting in the presence of noisy measurements. The hyper-parameter λ_2 determines the strength of the regularization of the model coefficients α and thus affects the sparsity of the resulting kernel function. If λ_2 is too large, the kernel function will be too simple and achieve poor forecasting; if it is too small, the function will be non-sparse and prone to overfitting. Both λ_1 and λ_2 should be chosen using k-fold cross-validation [17], which is a natural criterion for out-of sample forecasting, cf. below for more details. We'll fix $\tau = 5$ in our simulations but two methods were proposed in [26] to choose τ .

3 Simulations

In order to probe the generalization ability and the finite sample performance of the Sparse KFs algorithm, we apply our proposal to the dynamical system benchmarks comprising 132 chaotic dynamical systems in [19]. Furthermore, the proposed algorithm is compared to the baseline methods.

Benchmarks are computed on the High Performance Computing Platform of Nanjing University of Aeronautics and Astronautics, using Intel Xeon 8358 CPU and 256 GB RAM per node.

3.1 Data collection and performance criterion

The time series observations are collected by the precomputed time series on GitHub at <https://github.com/williamgilpin/dysts>. We use the default fine granularity setting by [19]. In this section, 7200 samples are generated for all systems to test the methods.

Given test samples $\{\mathbf{x}_k\}_{n+1}^N$ and the predictions $\{\hat{\mathbf{x}}_k\}_{n+1}^N$, the forecasting error is measured by two standard time series similarity metrics, symmetric mean absolute percentage error criterion (SMAPE) and Hausdorff Distance (HD) between the true attractor and the reconstructed attractor from data, respectively expressed as

$$\text{SMAPE}_{\text{test}}[\mathbf{x}] = \frac{1}{n} \sum_{i=1}^d \sum_{k=n+1}^N \frac{|\hat{x}_k^{(i)} - x_k^{(i)}|}{(|\hat{x}_k^{(i)}| + |x_k^{(i)}|)/2} \times 100\% \quad (7)$$

and

$$d_H(\hat{\mathbf{x}}, \mathbf{x}) = \max \left\{ \sup_{\hat{x} \in \hat{\mathbf{x}}} d(\hat{x}, \mathbf{x}), \sup_{x \in \mathbf{x}} d(\hat{\mathbf{x}}, x) \right\} \quad (8)$$

where $d(\hat{x}, \mathbf{x}) = \inf_{x \in \mathbf{x}} d(\hat{x}, x)$ quantifies the distance from a point $\hat{x} \in \hat{\mathbf{x}}$ to the subset $x \in \mathbf{x}$.

3.2 Experimental setting

Considering the computational efficiency and centre of this work, in all 132 dynamical systems, the embedding delay τ is set to 5, the shrinking parameter λ_1 is set to 0.05, and the sparsity

parameter λ_2 is determined by the 3-fold cross-validation [30]. In detail, splitting N samples into three part, for given values $\lambda_2 \in \{0, 0.0001, 0.001, 0.01, 0.1, 1, 10\}$, we learn the kernel on the observations of size $\frac{2}{3}N$ that remains when a contiguous block of $\frac{1}{3}N$ samples is removed. The left out samples then are "forecasted" by the learned kernel and compared to the true values. We repeat this procedure 3 times, and then compute the mean of the three SMAPEs of the results to get an average SMAPE for the 3-fold validation. Performing this cross-validation for each candidate value of the parameter set, we select the best one that leads to the smallest SMAPE over the forecasts. Note that $\lambda_2 = 0$ represents the Regular KFs scenario.

In addition to the hyper-parameters used in the objective function training, this algorithm requires an initial choice of base kernel functions. Here, in all 132 dynamical systems, we used a base kernel function that is a linear combination of 21 kernels:

$$\begin{aligned}
k_{\alpha, \theta} = & \alpha_1^2 (\mathbf{x}^\top \mathbf{y} + \theta_1^2) + \alpha_2^2 (\theta_2^2 \mathbf{x}^\top \mathbf{y} + \theta_3^2)^{|\theta_4|} + \alpha_3^2 \exp\left(\frac{-\|x - y\|_2^2}{2\theta_5^2}\right) + \alpha_4^2 \exp\left(\frac{-\|x - y\|_2}{2\theta_6^2}\right) \\
& + \alpha_5^2 \exp\left(\frac{-\sin^2(\pi\|x - y\|_2^2/\theta_7)}{\theta_8^2}\right) \exp\left(-\frac{\|x - y\|_2^2}{\theta_9^2}\right) + \alpha_6^2 \exp\left(\frac{-\sin^2(\pi\|x - y\|_2^2/\theta_{10})}{\theta_{11}^2}\right) \\
& + \alpha_7^2 \exp\left(\frac{-\sin^2(\pi\|x - y\|_2/\theta_{12})}{\theta_{13}^2}\right) \exp\left(-\frac{\|x - y\|_2}{\theta_{14}^2}\right) + \alpha_8^2 \exp\left(\frac{-\sin^2(\pi\|x - y\|_2/\theta_{15})}{\theta_{16}^2}\right) \\
& + \alpha_9^2 (\|x - y\|_2^2 + \theta_{17}^2)^{\frac{1}{2}} + \alpha_{10}^2 (\theta_{18}^2 + \theta_{19}^2 \|x - y\|_2^2)^{-\frac{1}{2}} + \alpha_{11}^2 (\theta_{20}^2 + \theta_{21}^2 \|x - y\|_2)^{-\frac{1}{2}} \\
& + \alpha_{12}^2 (\theta_{22}^2 + \|x - y\|_2)^{\theta_{23}} + \alpha_{13}^2 (\theta_{24}^2 + \|x - y\|_2^2)^{\theta_{25}} + \alpha_{14}^2 \left(1 + \left(\frac{\|x - y\|_2}{\theta_{26}}\right)^2\right)^{-1} \\
& + \alpha_{15}^2 \left(1 + \frac{\|x - y\|_2}{\theta_{27}}\right)^{-1} + \alpha_{16}^2 \left(1 - \frac{\|x - y\|_2^2}{\|x - y\|_2^2 + \theta_{28}^2}\right) \\
& + \alpha_{17}^2 \max\left(0, 1 - \frac{\|x - y\|_2^2}{\theta_{29}^2}\right) + \alpha_{18}^2 \max\left(0, 1 - \frac{\|x - y\|_2}{\theta_{30}^2}\right) \\
& + \alpha_{19}^2 (\log(\|x - y\|_2^{\theta_{31}} + 1)) + \alpha_{20}^2 \tanh(\theta_{32} \mathbf{x}^\top \mathbf{y} + \theta_{33}) \\
& + \alpha_{21}^2 \left[\arccos\left(-\frac{\|x - y\|_2}{\theta_{34}^2}\right) - \frac{\|x - y\|_2}{\theta_{34}^2} \sqrt{1 - \left(\frac{\|x - y\|_2}{\theta_{34}^2}\right)^2} \right] \cdot \mathbf{1}_{\{x, y: \|x - y\|_2^2 < \theta_{34}^2\}}
\end{aligned} \tag{9}$$

To further demonstrate the accuracy of the method, we make a comparison with several baseline methods, including kernel regression with Gaussian kernel ($\sigma = 1$) and trained Gaussian kernel by regular KFs, and regular KFs. For the convenience of presentation, kernel regression and trained Gaussian are abbreviated to "RBF", "Trained RBF", and "Regular", respectively.

3.3 Results

Sparsity penalty tuning. Figure 1 depicts the boxplots of the fitting errors obtained by Sparse KFs algorithm. Each box shows the distribution of forecast errors for all dynamical systems across different sparsity penalty. Taken as a whole, we observe that the forecasting error of Sparse

KFs is smaller than the regular one, indicating the superiority of the former to learning accurate representation of dynamical systems.

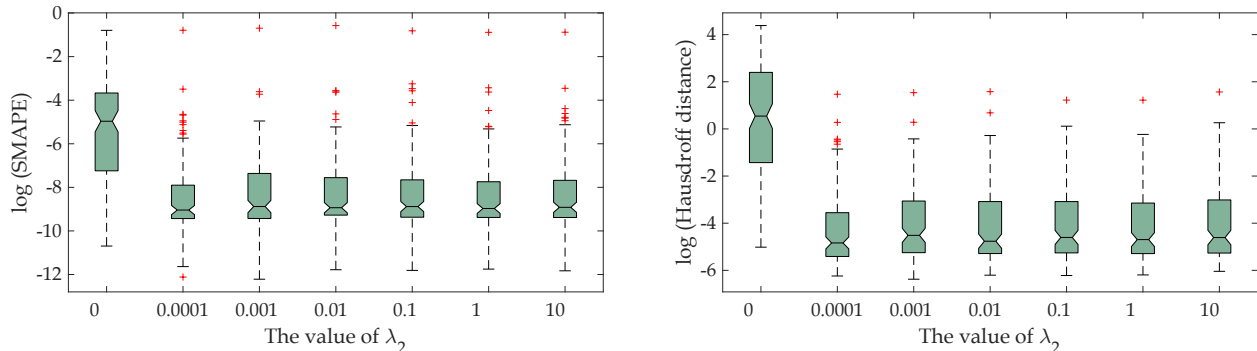


Figure 1: Distribution of forecasting errors for different sparsity penalty λ_2 for all 132 dynamical systems.

Visualization examples. In order to demonstrate the results intuitively, we present five examples here, including BeerRNN, Duffing, Double Pendulum, Lorenz and Lorenz Coupled systems. The fitting trajectories, loss iterations and learned weight coefficients obtained from Regular and Sparse KFs are summarized in Figure 2 and Table 1.

It is clear that in all cases, the identified trajectories by Sparse Kfs almost coincides with the true ones, although the test systems are chaotic. This phenomenon partially indicates the superiority of this kind of learning method for the reconstruction of the discrete maps. In addition, Table 1 shows that the weight coefficient obtained by the Regular Kfs are non-zeros, whereas the Sparse version gets sparsity weight coefficients, indicating the L_1 regularization penalty on α promotes sparsity in the resulting learned kernel function.

Comparison with baseline methods. Figure 3 and Table 2 show that comparison results with other baseline methods. On the basis of the results, we may roughly conclude the following: Figure 3 shows from the forecasting accuracy perspective, Sparse KFs outperforms RBF kernel, trained RBF kernel and regular KFs for almost all systems. In detail, in 128 systems, Sparse KFs has the smallest SMPEs and HDs, indicating adaptive kernel provides more precious forecasts. It is worth noting, however, that although Regular KFs shows slightly worse performance than RBF kernel and trained RBF kernel, it does not mean that Regular KFs is weaker. The reason for this phenomenon is that in the simulation conducted by using a large base kernel function, too many parameters lead to less robust and accurate results of Regular KFs. We also set the number of iterations for all methods to 7000 in order to make sure that they are being compared “fairly”.

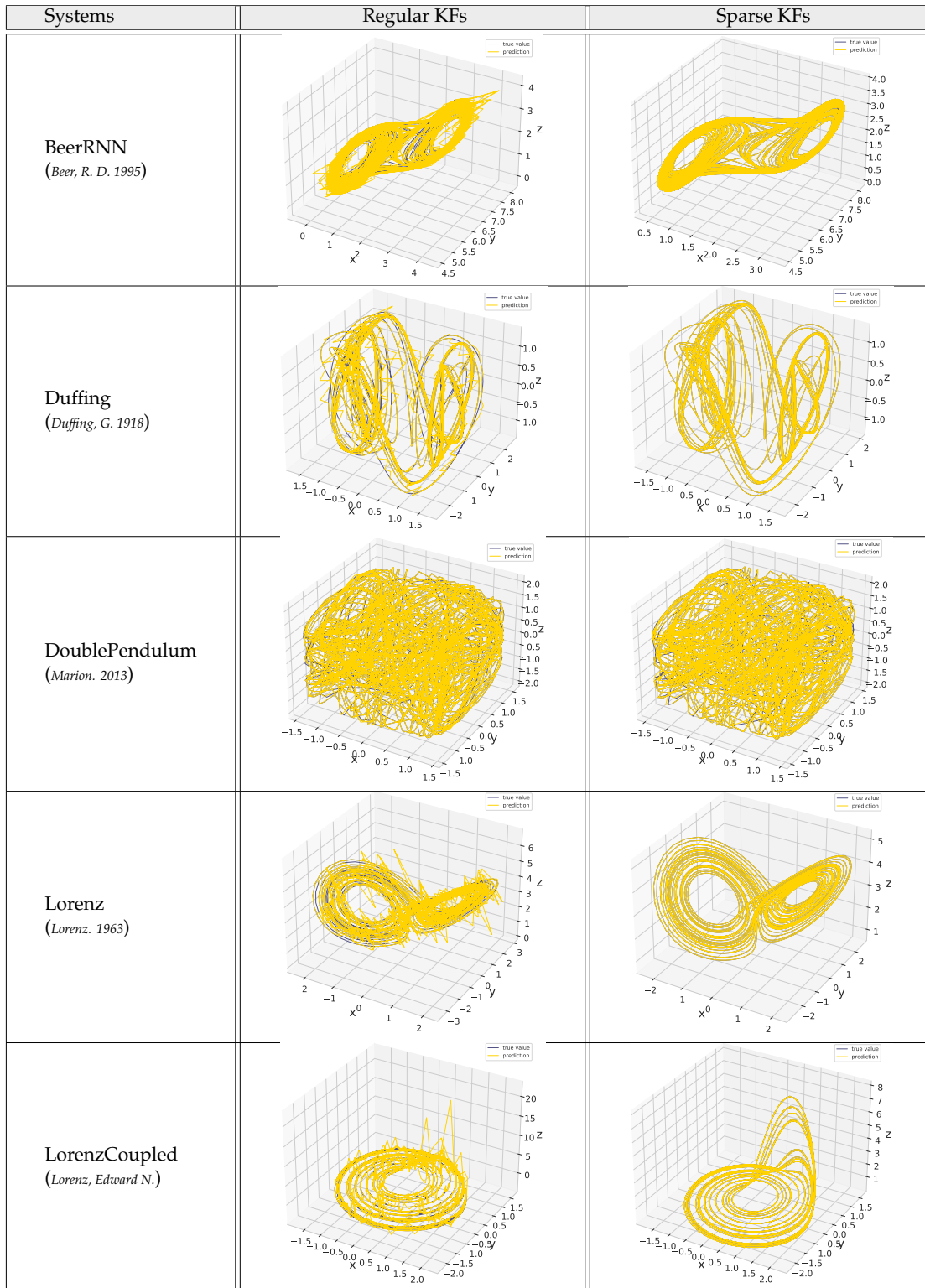


Figure 2: A comparison of learned phase plots for dynamical systems.

Table 1: Weight coefficients obtained by the Regular KFs and Sparse KFs

Coefficient	BeerRNN		Duffing		DoublePendulum		Lorenz		LorenzCoupled	
	Regular	Sparse	Regular	Sparse	Regular	Sparse	Regular	Sparse	Regular	Sparse
α_1	0.6739	0	0.7342	0	0.7363	0	0.7315	0	0.7347	0
α_2	0.7307	0.9985	0.7361	0.1606	0.7403	0.0242	0.7317	0.9918	0.7374	1
α_3	0.7248	0	0.7946	0.9970	0.7734	0.6807	0.7767	0	0.7545	0
α_4	0.7260	0	0.7853	0	0.7645	0	0.7629	0	0.7664	0
α_5	0.7188	0	0.7900	0.9839	0.7949	0	0.8256	0	0.7991	0
α_6	0.7703	0	0.6397	0	0.4591	0	0.7752	0	0.1696	0.9996
α_7	0.7190	0	0.7908	0.9878	0.8006	0	0.8168	0.2498	0.8249	0
α_8	0.7270	0	0.6572	0	0.5360	0	0.6986	0	0.6057	0
α_9	0.8214	0.9998	0.6476	0	0.6837	0	0.6893	0	0.7002	0
α_{10}	0.7282	0	0.7784	0	0.7613	0	0.7714	0	0.7552	0
α_{11}	0.7270	0	0.7637	0	0.7572	0	0.7634	0	0.7629	0
α_{12}	0.7307	0	0.7887	0	0.7774	0	0.7945	0.2785	0.7714	0
α_{13}	0.7307	0	0.7786	0	0.7746	0	0.7801	0	0.7856	0
α_{14}	0.7247	0	0.7887	0	0.7774	0	0.7945	0	0.7714	0
α_{15}	0.7241	0	0.7786	0	0.7746	0	0.7801	0	0.7856	0
α_{16}	0.7247	0	0.7887	0	0.7774	0	0.7945	0	0.7714	0
α_{17}	0.7189	0	0.7881	0	0.7950	0	0.7651	0	0.7994	0
α_{18}	0.7182	0	0.7884	0	0.8026	0	0.7545	0	0.8191	0
α_{19}	0.7308	0.8630	0.6017	0	0.6359	0	0.5834	0	0.6114	0
α_{20}	0.7307	1	0.1194	0	0.5472	0	0.5239	0	0.7272	0
α_{21}	0.7247	0	0.7311	0	0.7311	0	0.7311	0	0.7310	0

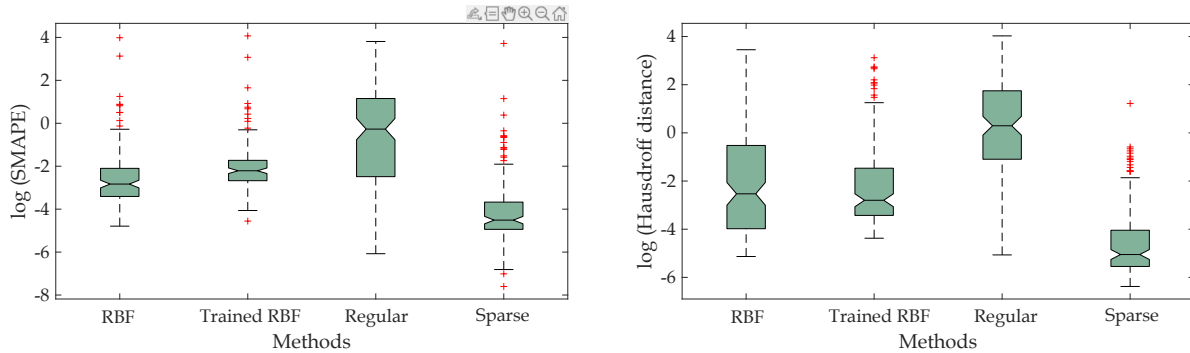


Figure 3: Distribution of forecasting errors for different methods for all 132 dynamical systems.

Table 2: one-head forecasting errors for 132 chaotic dynamical systems

Name	RBF Kernel		Trained RBF Kernel		Regular KFs		Sparse KFs		Best
	SMAPE	HD	SMAPE	HD	SMAPE	HD	SMAPE	HD	
Aizawa	0.0854	0.0151	0.2064	0.0253	0.0686	0.0530	0.0322	0.0027	Sparse KFs
AnishchenkoAstakhov	0.0528	0.3350	0.0771	0.0503	3.1902	3.7512	0.0082	0.0030	Sparse KFs
Arneodo	0.0596	0.0153	0.1155	0.0288	0.1310	0.5217	0.0103	0.0027	Sparse KFs
ArnoldBeltramiChildress	0.0899	0.0181	0.1424	0.0294	2.3615	2.1217	0.0764	0.0173	Sparse KFs
ArnoldWeb	2.2664	19.9685	0.7976	4.8003	1.0320	6.2204	0.0160	0.2081	Sparse KFs
AtmosphericRegime	0.5260	0.4882	0.6671	0.4404	3.1776	8.9202	0.5168	0.3314	Sparse KFs
BeerRNN	0.0501	0.9871	0.1005	0.1909	0.0169	0.0637	0.0048	0.0333	Sparse KFs
BelousovZhabotinsky	0.0587	10.5016	0.0839	8.0258	0.3797	0.5436	0.0096	0.0304	Sparse KFs
BickleyJet	0.0191	0.0246	0.0682	0.0606	0.8556	3.4248	0.0043	0.0065	Sparse KFs

continued on next page

continued from previous page

Name	RBF Kernel		Trained RBF Kernel		Regular KFs		Sparse KFs		
	SMAPE	HD	SMAPE	HD	SMAPE	HD	SMAPE	HD	Best
Blasius	0.0138	0.0390	0.0240	0.0524	0.0191	0.1562	0.0083	0.0061	Sparse KFs
BlinkingRotlet	0.5479	0.5731	0.7380	0.4513	6.5245	8.4845	0.2059	0.4307	Sparse KFs
BlinkingVortex	1.1316	0.5381	1.5324	0.5246	14.8773	42.3683	0.5423	0.5566	Trained RBF
Bouali	0.0411	0.3318	0.0914	0.1663	7.0934	10.6992	0.0057	0.0075	Sparse KFs
Bouali2	0.0278	0.2771	0.0396	0.0354	1.1552	5.1226	0.0034	0.0086	Sparse KFs
BurkeShaw	0.0964	0.9029	0.0730	0.1155	1.5393	2.0259	0.0099	0.0034	Sparse KFs
CaTwoPlus	0.0100	0.0601	0.0172	0.1073	0.0124	0.3303	0.0011	0.0119	Sparse KFs
CaTwoPlusQuasiperiodic	0.0169	0.0717	0.0278	0.1231	0.5585	3.2732	0.0005	0.0049	Sparse KFs
CellCycle	0.0914	2.6597	0.0434	0.4892	0.0504	0.9805	0.0049	0.0228	Sparse KFs
CellularNeuralNetwork	0.0623	0.0159	0.1102	0.0265	0.0369	0.0138	0.0326	0.0088	Sparse KFs
Chen	0.1159	1.5604	0.0665	0.2329	0.1607	0.3794	0.0125	0.0066	Sparse KFs
ChenLee	0.1110	0.0201	0.1627	0.0528	4.8465	2.9993	0.0075	0.0036	Sparse KFs
Chua	0.0567	0.0125	0.1087	0.0261	1.0280	0.8780	0.0031	0.0064	Sparse KFs
CircadianRhythm	0.0542	0.0616	0.1508	0.0431	3.4457	12.4484	0.1488	0.0418	Sparse KFs
CoevolvingPredatorPrey	0.1260	0.3105	0.3236	0.0719	0.0556	0.2102	0.0190	0.0460	Sparse KFs
Colpitts	0.0268	0.0908	0.0670	0.1956	0.0886	0.5858	0.0019	0.0339	Sparse KFs
Coulet	0.0435	0.0185	0.0947	0.0318	0.0038	0.0075	0.0031	0.0027	Sparse KFs
Dadras	0.6278	7.0971	0.4276	3.5036	1.5778	5.4706	0.0292	0.0218	Sparse KFs
DequanLi	0.1196	0.0140	0.1516	0.0347	0.0262	0.0157	0.0076	0.0034	Sparse KFs
DoubleGyre	0.0307	0.0171	0.0813	0.0372	2.3086	3.4297	0.0054	0.0077	Sparse KFs
DoublePendulum	0.7573	0.8038	0.6967	0.3224	0.6664	0.6741	0.7049	0.4731	Trained RBF
Duffing	0.0978	0.0784	0.1569	0.0395	2.2778	4.3408	0.0075	0.0043	Sparse KFs
ExcitableCell	0.0717	31.5628	0.0594	22.6648	0.0621	1.9013	0.0011	0.0125	Sparse KFs
Finance	0.0288	0.0871	0.0542	0.1120	0.4779	0.8187	0.0095	0.0062	Sparse KFs
FluidTrampoline	0.0849	0.0177	0.2124	0.0408	0.9629	0.9180	0.0076	0.0114	Sparse KFs
ForcedBrusselator	0.0177	0.0563	0.0375	0.0756	0.0231	0.1265	0.0036	0.0109	Sparse KFs
ForcedFitzHughNagumo	0.0478	0.0106	0.1107	0.0225	3.1649	12.5503	0.0595	0.0363	RBF kernel
ForcedVanDerPol	0.0702	0.1656	0.1793	0.0893	32.2307	11.5199	0.1758	0.0333	Sparse KFs
GenesioTesi	0.0272	0.0110	0.0687	0.0236	0.0455	0.0460	0.0099	0.0035	Sparse KFs
GuckenheimerHolmes	0.0589	0.0119	0.1995	0.0126	2.2780	1.7778	0.0113	0.0021	Sparse KFs
Hadley	0.0193	0.0144	0.0592	0.0265	6.9133	12.1686	0.0070	0.0027	Sparse KFs
Halvorsen	0.0331	0.0134	0.0810	0.0274	0.1418	0.1032	0.0163	0.0036	Sparse KFs
HastingsPowell	0.0111	0.0522	0.0200	0.0898	0.2947	1.7779	0.0039	0.0093	Sparse KFs
HenonHeiles	0.0553	0.0120	0.1538	0.0333	0.3714	0.4323	0.0262	0.0020	Sparse KFs
HindmarshRose	0.0622	0.2604	0.1585	0.1188	1.4425	3.1906	0.0501	0.0121	Sparse KFs
Hopfield	0.1021	0.0324	0.1919	0.0592	0.1754	0.2280	0.0683	0.0816	RBF kernel
HyperBao	0.0399	0.1957	0.0829	0.1004	0.7975	0.3617	0.0020	0.0062	Sparse KFs
HyperCai	0.0212	0.0389	0.0714	0.0693	0.8580	2.4500	0.0073	0.0072	Sparse KFs
HyperJha	0.0320	0.0810	0.0886	0.0532	0.0101	0.0434	0.0091	0.0055	Sparse KFs
HyperLorenz	0.1537	0.6141	0.1876	0.1559	0.4916	2.6555	0.0216	0.0060	Sparse KFs
HyperLu	0.0454	0.2597	0.0692	0.0618	2.4988	5.8150	0.0074	0.0061	Sparse KFs
HyperPang	0.0515	0.3774	0.1154	0.1149	5.1907	13.6200	0.0182	0.0070	Sparse KFs
HyperQi	2.4233	16.5116	2.1187	15.3750	0.0328	0.1830	0.0096	0.0042	Sparse KFs
HyperRossler	0.1849	4.9064	0.1403	2.1973	7.9312	3.6411	0.0321	0.0066	Sparse KFs
HyperWang	0.1120	2.2110	0.1174	0.1792	0.3002	2.5751	0.0069	0.0047	Sparse KFs
HyperXu	0.3531	6.3933	0.2033	1.0195	2.2529	14.5259	0.0197	0.0077	Sparse KFs
HyperYan	0.4243	10.1189	0.4279	7.9264	0.0586	0.9171	0.0104	0.0037	Sparse KFs
HyperYangChen	0.1246	2.0286	0.1526	0.6631	3.1985	7.6886	0.0247	0.0066	Sparse KFs
IkedaDelay	0.2180	0.1746	0.2381	0.1818	0.4705	0.1368	0.2961	0.0856	Sparse KFs
IsothermalChemical	0.0102	0.1364	0.0189	0.2037	0.0306	0.3389	0.0018	0.0127	Sparse KFs
ItikBanksTumor	3.4911	0.0366	5.2174	0.0569	16.1445	0.4902	1.4649	0.0033	Sparse KFs
JerkCircuit	0.2601	1.1662	0.3421	1.1248	1.7674	3.4755	0.0815	0.2651	Sparse KFs

continued on next page

continued from previous page

Name	RBF Kernel		Trained RBF Kernel		Regular KFs		Sparse KFs		
	SMAPE	HD	SMAPE	HD	SMAPE	HD	SMAPE	HD	Best
KawczynskiStrizhak	0.0199	0.0087	0.0409	0.0157	0.0167	0.1762	0.0029	0.0062	Sparse KFs
Laser	0.0590	0.0146	0.0985	0.0310	1.7385	1.1979	0.0046	0.0039	Sparse KFs
LiuChen	53.8448	10.6533	58.6287	9.0421	45.1807	56.0694	41.2576	0.5160	Sparse KFs
Lorenz	0.0245	0.0534	0.0607	0.0590	0.2986	5.6588	0.0097	0.0056	Sparse KFs
Lorenz84	0.1106	0.0208	0.2197	0.0367	5.5515	9.8087	0.0198	0.0047	Sparse KFs
Lorenz96	0.2024	0.1248	0.2927	0.0854	0.1325	0.0938	0.0682	0.0069	Sparse KFs
LorenzBounded	0.0333	0.0203	0.0654	0.0419	3.1867	4.2336	0.0108	0.0042	Sparse KFs
LorenzCoupled	0.1911	2.2629	0.1561	0.4420	0.1409	1.0359	0.0106	0.0077	Sparse KFs
LorenzStenflo	0.0614	0.7118	0.1174	0.1737	0.2002	1.6822	0.0236	0.0075	Sparse KFs
LuChen	0.0275	0.1926	0.0517	0.0634	0.1885	0.2325	0.0112	0.0068	Sparse KFs
LuChenCheng	0.0256	0.0155	0.0716	0.0342	0.0470	0.0344	0.0048	0.0036	Sparse KFs
MacArthur	0.2159	3.7403	0.1198	0.9447	1.8603	13.9467	0.0120	0.2382	Sparse KFs
MackeyGlass	0.1206	1.2080	0.0532	0.2552	0.0293	0.3855	0.0211	0.0713	Sparse KFs
MooreSpiegel	0.0678	0.0196	0.0997	0.0327	0.0708	0.0337	0.0120	0.0044	Sparse KFs
MultiChua	0.0305	0.0189	0.0605	0.0335	0.0044	0.0095	0.0074	0.0079	Sparse KFs
NewtonLiepnik	0.0389	0.0599	0.0726	0.0612	4.5397	7.8006	0.0080	0.0064	Sparse KFs
NoseHoover	0.0689	0.0808	0.1300	0.0533	0.1955	1.6547	0.0168	0.0031	Sparse KFs
NuclearQuadrupole	0.0362	0.0100	0.1274	0.0295	10.1185	24.2304	0.0087	0.0035	Sparse KFs
OscillatingFlow	0.1049	0.0517	0.2193	0.0740	6.0614	21.8075	0.1080	0.0362	Sparse KFs
PanXuZhou	0.0545	0.0339	0.0758	0.0548	0.0023	0.0063	0.0104	0.0046	Sparse KFs
PehlivanWei	0.0452	0.0618	0.0975	0.0399	1.1849	1.4213	0.0122	0.0027	Sparse KFs
PiecewiseCircuit	1.6576	2.1655	1.0962	1.1540	15.2214	43.3544	0.4094	0.3498	Sparse KFs
Qi	0.4800	17.9306	0.1886	6.2674	0.8552	1.0737	0.0414	0.0185	Sparse KFs
QiChen	0.0212	0.4044	0.0377	0.0764	2.1510	3.6610	0.0137	0.0099	Sparse KFs
RabinovichFabrikant	0.0192	0.0217	0.0436	0.0443	0.2219	0.3756	0.0061	0.0046	Sparse KFs
RayleighBenard	0.0331	0.4220	0.0476	0.0894	1.9415	8.8976	0.0087	0.0067	Sparse KFs
RikitakeDynamo	0.2219	3.3427	0.0909	0.3441	6.6172	8.6545	0.0101	0.0042	Sparse KFs
Rossler	0.0733	0.3618	0.1233	0.2284	5.5017	0.7442	0.0295	0.0045	Sparse KFs
Rucklidge	0.0663	0.2276	0.0939	0.1333	1.1506	1.2679	0.0142	0.0053	Sparse KFs
Sakarya	0.4167	4.6813	0.1509	0.5028	18.0913	42.2980	0.0154	0.0050	Sparse KFs
SaltonSea	0.0106	0.0308	0.0192	0.0592	0.0649	0.5014	0.0009	0.0039	Sparse KFs
SanUmSrisuchinwong	0.0693	0.0841	0.1640	0.0393	0.4196	0.6232	0.0172	0.0086	Sparse KFs
ScrollDelay	0.2267	0.0875	0.4362	0.0730	0.3276	0.1406	0.3249	0.1553	Trained RBF
ShimizuMorioka	0.0287	0.0250	0.0735	0.0445	0.1192	0.3879	0.0128	0.0048	Sparse KFs
SprottA	0.0792	0.0214	0.1122	0.0216	0.8126	0.9618	0.0150	0.0033	Sparse KFs
SprottB	0.2469	2.4581	0.1138	0.8743	0.4810	1.7777	0.0108	0.0039	Sparse KFs
SprottC	0.0587	0.0301	0.0925	0.0300	8.2328	11.7319	0.0074	0.0032	Sparse KFs
SprottD	0.0302	0.2308	0.0723	0.0541	0.0425	0.3622	0.0071	0.0048	Sparse KFs
SprottDelay	0.0083	0.0076	0.0105	0.0141	0.0294	0.0434	0.0018	0.0050	Sparse KFs
SprottE	0.0469	0.0669	0.0825	0.0302	0.1184	0.5445	0.0124	0.0042	Sparse KFs
SprottF	0.0596	0.0140	0.1045	0.0226	2.3749	1.4670	0.0083	0.0046	Sparse KFs
SprottG	0.0488	0.0142	0.1028	0.0311	0.0649	0.0432	0.0155	0.0034	Sparse KFs
SprottH	0.0656	0.0629	0.1767	0.0575	6.8195	11.4266	0.0178	0.0051	Sparse KFs
SprottI	0.0227	0.0117	0.0550	0.0228	0.4148	1.5234	0.0055	0.0038	Sparse KFs
SprottJ	0.0220	0.0087	0.0475	0.0208	0.3507	0.4144	0.0090	0.0031	Sparse KFs
SprottJerk	0.0487	0.0163	0.1089	0.0213	0.0794	0.0215	0.0149	0.0042	Sparse KFs
SprottK	0.0794	0.0225	0.1289	0.0295	1.4930	2.0306	0.0095	0.0030	Sparse KFs
SprottL	0.0183	0.0233	0.0375	0.0481	0.0228	0.1415	0.0059	0.0083	Sparse KFs
SprottM	0.0415	0.0135	0.0628	0.0266	0.0221	0.1329	0.0094	0.0034	Sparse KFs
SprottMore	1.6479	0.4151	1.9667	0.4853	10.3418	16.8864	0.3135	0.3061	Sparse KFs
SprottN	0.0437	0.0059	0.1139	0.0141	3.1838	0.8044	0.0201	0.0035	Sparse KFs
SprottO	0.0381	0.0129	0.0816	0.0265	0.4222	0.3765	0.0120	0.0024	Sparse KFs

continued on next page

continued from previous page

Name	RBF Kernel		Trained RBF Kernel		Regular KFs		Sparse KFs		
	SMAPE	HD	SMAPE	HD	SMAPE	HD	SMAPE	HD	Best
SprottP	0.0537	0.0115	0.0956	0.0246	1.7639	1.4943	0.0065	0.0018	Sparse KFs
SprottQ	0.0421	0.0117	0.0835	0.0218	0.0725	0.1081	0.0037	0.0017	Sparse KFs
SprottR	0.0512	0.2892	0.1037	0.0323	0.0206	0.0214	0.0122	0.0046	Sparse KFs
SprottS	0.0492	0.0146	0.1321	0.0283	1.4998	1.1302	0.0072	0.0033	Sparse KFs
SprottTorus	0.8820	10.3824	0.4914	7.2845	1.7149	10.1249	0.0068	0.0262	Sparse KFs
StickSlipOscillator	0.0347	0.0222	0.0899	0.0627	0.0873	0.1241	0.0025	0.0032	Sparse KFs
SwingingAtwood	0.5239	3.8956	0.2178	0.6361	5.4253	43.2463	0.0878	0.3789	Sparse KFs
Thomas	0.0557	0.0084	0.1331	0.0172	7.1262	8.0657	0.0188	0.0074	Sparse KFs
ThomasLabyrinth	0.5695	0.1802	1.2520	0.1557	15.4092	19.7441	0.5611	0.2008	Trained RBF
Torus	0.0090	0.0542	0.0253	0.1119	0.0091	0.0356	0.0037	0.0104	Sparse KFs
Tsucs2	0.0640	0.2447	0.1171	0.0331	1.2793	0.4068	0.0276	0.0051	Sparse KFs
TurchinHanski	0.0604	0.1802	0.1381	0.0422	0.7294	0.8868	0.0247	0.0178	Sparse KFs
VallisElNino	0.0300	0.0136	0.0610	0.0206	0.0358	0.0140	0.0118	0.0037	Sparse KFs
VossDelay	22.8701	14.9384	21.5940	14.3340	8.1493	9.6495	3.1540	3.3905	Sparse KFs
WangSun	0.6255	6.2263	0.5542	4.3660	0.1105	2.4657	0.0394	0.0252	Sparse KFs
WindmiReduced	0.0989	1.5788	0.1263	1.8788	0.1129	1.8904	0.0096	0.2036	Sparse KFs
YuWang	0.0497	0.4307	0.1203	0.2755	7.2926	36.7611	0.1190	0.0828	Sparse KFs
YuWang2	0.0249	0.0269	0.0402	0.0458	2.3506	2.0104	0.0051	0.0128	Sparse KFs
ZhouChen	2.3689	21.1758	2.5197	15.2920	12.8991	27.8790	0.2194	0.0134	Sparse KFs

4 Conclusion

In this work, we present a Sparse Kernel Flows algorithm for learning the ‘best’ kernel from data. The proposal provides an effective modification of the method of Regular Kernel Flows that allows sparsifying the initial base kernel and improves the accuracy. Our numerical experiments on a benchmark of 132 chaotic systems demonstrate that the learned kernel using Sparse Kernel Flows is able to accurately represent the underlying dynamical system responsible for generating the time series data.

Acknowledgment

This research was completed during the first author’s visit to Imperial College London; L.Y. thanks Boumediene Hamzi and Jeroen Lamb for hosting the visit. L.Y. thanks the Nanjing University of Aeronautics and Astronautics for funding through Interdisciplinary Innovation Fund for Doctoral Students KXCXJJ202208. Naiming Xie acknowledges support from the National Natural Science Foundation of China (72171116), and the Fundamental Research Funds for the Central Universities of China (NP2020022). HO acknowledges support from the Air Force Office of Scientific Research under MURI award number FA9550-20-1-0358 (Machine Learning and Physics-Based Modeling and Simulation) and the Department of Energy under the MMICCs SEA-CROGS award. BH acknowledges support from the Air Force Office of Scientific Research (award number FA9550-21-1-0317) and the Department of Energy (award number SA22-0052-S001).

A Appendix

A.1 Reproducing Kernel Hilbert Spaces (RKHS)

We give a brief overview of reproducing kernel Hilbert spaces as used in statistical learning theory [13]. Early work developing the theory of RKHS was undertaken by N. Aronszajn [4].

Definition 1. Let \mathcal{H} be a Hilbert space of functions on a set \mathcal{X} . Denote by $\langle f, g \rangle$ the inner product on \mathcal{H} and let $\|f\| = \langle f, f \rangle^{1/2}$ be the norm in \mathcal{H} , for f and $g \in \mathcal{H}$. We say that \mathcal{H} is a reproducing kernel Hilbert space (RKHS) if there exists a function $k : \mathcal{X} \times \mathcal{X} \rightarrow \mathbb{R}$ such that

- i. $k_x := k(x, \cdot) \in \mathcal{H}$ for all $x \in \mathcal{X}$.
- ii. k spans \mathcal{H} : $\mathcal{H} = \overline{\text{span}\{k_x \mid x \in \mathcal{X}\}}$.
- iii. k has the reproducing property: $\forall f \in \mathcal{H}, f(x) = \langle f, k_x \rangle$.

k will be called a reproducing kernel of \mathcal{H} . \mathcal{H}_k will denote the RKHS \mathcal{H} with reproducing kernel k where it is convenient to explicitly note this dependence.

The important properties of reproducing kernels are summarized in the following proposition.

Proposition 1. If k is a reproducing kernel of a Hilbert space \mathcal{H} , then

- i. $k(x, y)$ is unique.
- ii. $\forall x, y \in \mathcal{X}, k(x, y) = k(y, x)$ (symmetry).
- iii. $\sum_{i,j=1}^q \alpha_i \alpha_j k(x_i, x_j) \geq 0$ for $\alpha_i \in \mathbb{R}, x_i \in \mathcal{X}$ and $q \in \mathbb{N}_+$ (positive definiteness).
- iv. $\langle k(x, \cdot), k(y, \cdot) \rangle = K(x, y)$.

Common examples of reproducing kernels defined on a compact domain $\mathcal{X} \subset \mathbb{R}^n$ are the (1) constant kernel: $K(x, y) = m > 0$ (2) linear kernel: $k(x, y) = x \cdot y$ (3) polynomial kernel: $k(x, y) = (1 + x \cdot y)^d$ for $d \in \mathbb{N}_+$ (4) Laplace kernel: $k(x, y) = e^{-\|x-y\|_2/\sigma^2}$, with $\sigma > 0$ (5) Gaussian kernel: $k(x, y) = e^{-\|x-y\|_2^2/\sigma^2}$, with $\sigma > 0$ (6) triangular kernel: $k(x, y) = \max\{0, 1 - \frac{\|x-y\|_2}{\sigma}\}$, with $\sigma > 0$. (7) locally periodic kernel: $k(x, y) = \sigma^2 e^{-2\frac{\sin^2(\pi\|x-y\|_2/p)}{\ell^2}} e^{-\frac{\|x-y\|_2^2}{2\ell^2}}$, with $\sigma, \ell, p > 0$.

Theorem 1. Let $k : \mathcal{X} \times \mathcal{X} \rightarrow \mathbb{R}$ be a symmetric and positive definite function. Then there exists a Hilbert space of functions \mathcal{H} defined on \mathcal{X} admitting k as a reproducing Kernel. Conversely, let \mathcal{H} be a Hilbert space of functions $f : \mathcal{X} \rightarrow \mathbb{R}$ satisfying $\forall x \in \mathcal{X}, \exists \kappa_x > 0$, such that $|f(x)| \leq \kappa_x \|f\|_{\mathcal{H}}, \forall f \in \mathcal{H}$. Then \mathcal{H} has a reproducing kernel k .

Theorem 2. Let $k(x, y)$ be a positive definite kernel on a compact domain or a manifold X . Then there exists a Hilbert space \mathcal{F} and a function $\Phi : X \rightarrow \mathcal{F}$ such that

$$k(x, y) = \langle \Phi(x), \Phi(y) \rangle_{\mathcal{F}} \quad \text{for } x, y \in X.$$

Φ is called a feature map, and \mathcal{F} a feature space².

²The dimension of the feature space can be infinite, for example in the case of the Gaussian kernel.

Data accessibility

Data and codes are available at https://github.com/Yanglu0319/Sparse_Kernel_Flows.

References

- [1] Abarbanel, H., 2012. Analysis of Observed Chaotic Data. Institute for Nonlinear Science, Springer New York.
- [2] Akian, J.L., Bonnet, L., Owhadi, H., Savin, É., 2022. Learning “best” kernels from data in Gaussian process regression. With application to aerodynamics. *Journal of Computational Physics* 470, 111595. doi:[10.1016/j.jcp.2022.111595](https://doi.org/10.1016/j.jcp.2022.111595).
- [3] Alexander, R., Giannakis, D., 2020. Operator-theoretic framework for forecasting nonlinear time series with kernel analog techniques. *Physica D: Nonlinear Phenomena* 409, 132520. URL: <http://www.sciencedirect.com/science/article/pii/S016727891930377X>, doi:<https://doi.org/10.1016/j.physd.2020.132520>.
- [4] Aronszajn, N., 1950. Theory of reproducing kernels. *Transactions of the American Mathematical Society* 68, 337–404. URL: <http://dx.doi.org/10.2307/1990404>.
- [5] Bottou, L., 2012. Stochastic Gradient Descent Tricks, in: Montavon, G., Orr, G.B., Müller, K.R. (Eds.), *Neural Networks: Tricks of the Trade: Second Edition*. Springer, Berlin, Heidelberg. *Lecture Notes in Computer Science*, pp. 421–436. doi:[10.1007/978-3-642-35289-8_25](https://doi.org/10.1007/978-3-642-35289-8_25).
- [6] Bouvrie, J., Hamzi, B., 2012. Empirical estimators for stochastically forced nonlinear systems: Observability, controllability and the invariant measure. *Proc. of the 2012 American Control Conference*, 294–301 <https://arxiv.org/abs/1204.0563v1>.
- [7] Bouvrie, J., Hamzi, B., 2017a. Kernel methods for the approximation of nonlinear systems. *SIAM J. Control and Optimization* <https://arxiv.org/abs/1108.2903>.
- [8] Bouvrie, J., Hamzi, B., 2017b. Kernel methods for the approximation of some key quantities of nonlinear systems. *Journal of Computational Dynamics* 1. <http://arxiv.org/abs/1204.0563>.
- [9] Brunton, S.L., Proctor, J.L., Kutz, J.N., 2016. Discovering governing equations from data by sparse identification of nonlinear dynamical systems. *Proceedings of the National Academy of Sciences* 113, 3932–3937. URL: <https://www.pnas.org/content/113/15/3932>, doi:[10.1073/pnas.1517384113](https://doi.org/10.1073/pnas.1517384113), [arXiv:https://www.pnas.org/content/113/15/3932.full.pdf](https://arxiv.org/abs/1204.0563).
- [10] Casdagli, M., 1989. Nonlinear prediction of chaotic time series. *Physica D: Nonlinear Phenomena* 35, 335–356. URL: <http://www.sciencedirect.com/science/article/pii/0167278989900742>, doi:[https://doi.org/10.1016/0167-2789\(89\)90074-2](https://doi.org/10.1016/0167-2789(89)90074-2).
- [11] Chattopadhyay, A., Hassanzadeh, P., Palem, K.V., Subramanian, D., 2019. Data-driven prediction of a multi-scale Lorenz 96 chaotic system using a hierarchy of deep learning methods: Reservoir computing, ANN, and RNN-LSTM. *CoRR* abs/1906.08829. URL: <http://arxiv.org/abs/1906.08829>, [arXiv:1906.08829](https://arxiv.org/abs/1906.08829).
- [12] Chen, Y., Hosseini, B., Owhadi, H., Stuart, A.M., 2021. Solving and learning nonlinear PDEs with Gaussian processes. *Journal of Computational Physics* 447, 110668. doi:[10.1016/j.jcp.2021.110668](https://doi.org/10.1016/j.jcp.2021.110668).
- [13] Cucker, F., Smale, S., 2002. On the mathematical foundations of learning. *Bulletin of the American Mathematical Society* 39, 1–49.
- [14] Darcy, M., Hamzi, B., Susiluoto, J., Braverman, A., Owhadi, H., 2023. Learning dynamical systems from data: a simple cross-validation perspective, part II: nonparametric kernel flows. *Physica D* 444, 133583. URL: https://www.researchgate.net/publication/356818178_Learning_dynamical_systems_from_data_a_simple_cross-validation_perspective_part_II_nonparametric_kernel_flows.
- [15] Darcy, M., Tavallali, P., Livieri, G., Hamzi, B., Owhadi, H., 2021. One-shot

- learning of stochastic differential equations with computational graph completion. preprint URL: https://www.researchgate.net/profile/Boumediene-Hamzi/publication/358263232_One-Shot_Learning_of_Stochastic_Differential_Equations_with_Computational_Graph_Completion/links/61f8fd2b11a1090a79c707ca/One-Shot-Learning-of-Stochastic-Differential-Equations-with-Computational-Graph-Completion.pdf.
- [16] D.Wittwar, B.B.G., 2021. Kernel methods for center manifold approximation and a weak data-based version of the center manifold theorems. *Physica D*.
- [17] Exterkate, P., Groenen, P.J.F., Heij, C., van Dijk, D., 2016. Nonlinear forecasting with many predictors using kernel ridge regression. *International Journal of Forecasting* 32, 736–753. doi:[10.1016/j.ijforecast.2015.11.017](https://doi.org/10.1016/j.ijforecast.2015.11.017).
- [18] Giesl, P., Hamzi, B., Rasmussen, M., Webster, K., 2019. Approximation of Lyapunov functions from noisy data. *Journal of Computational Dynamics* doi:[10.3934/jcd.2020003](https://doi.org/10.3934/jcd.2020003). <https://arxiv.org/abs/1601.01568>.
- [19] Gilpin, W., 2021. Chaos as an interpretable benchmark for forecasting and data-driven modelling. [arXiv:2110.05266](https://arxiv.org/abs/2110.05266).
- [20] González-García, R., Rico-Martínez, R., Kevrekidis, I., 1998. Identification of distributed parameter systems: A neural net based approach. *Computers & Chemical Engineering* 22, S965–S968. URL: <https://www.sciencedirect.com/science/article/pii/S0098135498001914>, doi:[https://doi.org/10.1016/S0098-1354\(98\)00191-4](https://doi.org/10.1016/S0098-1354(98)00191-4). european Symposium on Computer Aided Process Engineering-8.
- [21] Grandstrand, O., 1995. Nonlinear system identification using neural networks: dynamics and instabilities, in: Bulsari, A.B. (Ed.), *Neural Networks for Chemical Engineers*. Elsevier, Elsevier. chapter 16, pp. 409–442.
- [22] Haasdonk, B., Hamzi, B., Santin, G., Wittwar, D., 2018. Greedy kernel methods for center manifold approximation. *Proc. of ICOSAHOM 2018, International Conference on Spectral and High Order Methods* <https://arxiv.org/abs/1810.11329>.
- [23] Hamzi, B., Colonus, F., 2019. Kernel methods for the approximation of discrete-time linear autonomous and control systems. *SN Applied Sciences* 1, 674. doi:[10.1007/s42452-019-0701-3](https://doi.org/10.1007/s42452-019-0701-3).
- [24] Hamzi, B., Kuehn, C., Mohamed, S., 2019. A note on kernel methods for multiscale systems with critical transitions. *Mathematical Methods in the Applied Sciences* 42, 907–917. URL: <https://onlinelibrary.wiley.com/doi/abs/10.1002/mma.5394>, doi:<https://doi.org/10.1002/mma.5394>, [arXiv:https://onlinelibrary.wiley.com/doi/pdf/10.1002/mma.5394](https://onlinelibrary.wiley.com/doi/pdf/10.1002/mma.5394).
- [25] Hamzi, B., Maulik, R., Owhadi, H., 2022. Simple, low-cost and accurate data-driven geophysical forecasting with learned kernels. *Proceedings of the Royal Society A: Mathematical, Physical and Engineering Sciences*, 18.
- [26] Hamzi, B., Owhadi, H., 2021a. Learning dynamical systems from data: A simple cross-validation perspective, part i: Parametric kernel flows. *Physica D: Nonlinear Phenomena* 421, 132817. URL: <https://www.sciencedirect.com/science/article/pii/S0167278920308186>, doi:<https://doi.org/10.1016/j.physd.2020.132817>.
- [27] Hamzi, B., Owhadi, H., 2021b. Learning dynamical systems from data: A simple cross-validation perspective, part I: Parametric kernel flows. *Physica D: Nonlinear Phenomena* 421, 132817. doi:[10.1016/j.physd.2020.132817](https://doi.org/10.1016/j.physd.2020.132817).
- [28] Hamzi, B., Owhadi, H., Kevrekidis, Y., 2023. Learning dynamical systems from data: A simple cross-validation perspective, part iv: case with partial observations.
- [29] Hudson, J., Kube, M., Adomaitis, R., Kevrekidis, I., Lapedes, A., Farber, R., 1990. Nonlinear signal processing and system identification: applications to time series from electrochemical reactions. *Chemical Engineering Science* 45, 2075–2081. URL: <https://www.sciencedirect.com/science/article/pii/>

000925099080079T, doi:[https://doi.org/10.1016/0009-2509\(90\)80079-T](https://doi.org/10.1016/0009-2509(90)80079-T).

- [30] Jung, Y., 2018. Multiple predicting K-fold cross-validation for model selection. *Journal of Nonparametric Statistics* 30, 197–215. doi:[10.1080/10485252.2017.1404598](https://doi.org/10.1080/10485252.2017.1404598).
- [31] Kantz, H., Schreiber, T., 1997. *Nonlinear Time Series Analysis*. Cambridge University Press, USA.
- [32] Klus, S., Nüske, F., Hamzi, B., 2020a. Kernel-based approximation of the koopman generator and schrödinger operator. *Entropy* 22, 722.
- [33] Klus, S., Nuske, F., Hamzi, B., 2020b. Kernel-based approximation of the koopman generator and schrödinger operator. *Entropy* 22. <https://www.mdpi.com/1099-4300/22/7/722>.
- [34] Klus, S., Nüske, F., Peitz, S., Niemann, J.H., Clementi, C., Schütte, C., 2020c. Data-driven approximation of the koopman generator: Model reduction, system identification, and control. *Physica D: Nonlinear Phenomena* 406, 132416.
- [35] Koltai, A.B.S.K.B.H.P., Schutte, C., 2019. Dimensionality reduction of complex metastable systems via kernel embeddings of transition manifold. <https://arxiv.org/abs/1904.08622>.
- [36] Lee, J., De Brouwer, E., Hamzi, B., Owhadi, H., 2021. Learning dynamical systems from data: A simple cross-validation perspective, part III: Irregularly-Sampled Time Series. [arXiv:2111.13037](https://arxiv.org/abs/2111.13037).
- [37] Lu, Y., Hamzi, B., Owhadi, H., Kevrekidis, Y., Xiuwen, S., Naiming, X., 2023. Learning dynamical systems from data: A simple cross-validation perspective, part vii: Hausdroff distance .
- [38] Nielsen, A., 2019. *Practical Time Series Analysis: Prediction with Statistics and Machine Learning*. O'Reilly Media.
- [39] Owhadi, B.H.R.M.H., 2021a. Simple, low-cost and accurate data-driven geophysical forecasting with learned kernels. *Proceedings of the Royal Society A: Mathematical, Physical and Engineering Sciences* 477(2252). doi:[10.1098/rspa.2021.0326](https://doi.org/10.1098/rspa.2021.0326).
- [40] Owhadi, H., 2021b. Computational graph completion URL: <https://arxiv.org/abs/2110.10323>, doi:[10.48550/ARXIV.2110.10323](https://doi.org/10.48550/ARXIV.2110.10323).
- [41] Owhadi, H., Scovel, C., 2019. *Operator-Adapted Wavelets, Fast Solvers, and Numerical Homogenization: from a game theoretic approach to numerical approximation and algorithm design*. Cambridge Monographs on Applied and Computational Mathematics, Cambridge University Press.
- [42] Owhadi, H., Yoo, G.R., 2019a. Kernel flows: From learning kernels from data into the abyss. *Journal of Computational Physics* 389, 22–47. doi:[10.1016/j.jcp.2019.03.040](https://doi.org/10.1016/j.jcp.2019.03.040).
- [43] Owhadi, H., Yoo, G.R., 2019b. Kernel Flows: From learning kernels from data into the abyss. *Journal of Computational Physics* 389, 22–47. doi:[10.1016/j.jcp.2019.03.040](https://doi.org/10.1016/j.jcp.2019.03.040).
- [44] Pathak, J., Lu, Z., Hunt, B.R., Girvan, M., Ott, E., 2017. Using machine learning to replicate chaotic attractors and calculate lyapunov exponents from data. *Chaos: An Interdisciplinary Journal of Nonlinear Science* 27, 121102. URL: <https://doi.org/10.1063/1.5010300>, doi:[10.1063/1.5010300](https://doi.org/10.1063/1.5010300).
- [45] Rico-Martinez, R., Krischer, K., Kevrekidis, I., Kube, M., Hudson, J., 1992. Discrete-vs. continuous-time nonlinear signal processing of cu electrodisolution data. *Chemical Engineering Communications* 118, 25–48.
- [46] Santin, G., Haasdonk, B., 2019. Kernel methods for surrogate modeling <https://arxiv.org/abs/1907.105566>.
- [47] Tibshirani, R., 1996. Regression Shrinkage and Selection Via the Lasso. *Journal of the Royal Statistical Society: Series B (Methodological)* 58, 267–288. doi:[10.1111/j.2517-6161.1996.tb02080.x](https://doi.org/10.1111/j.2517-6161.1996.tb02080.x).
- [48] Yasamin, J., Hamzi, B., Owhadi, H., Peyman, T., Moustafa, S., 2023. Learning dynamical systems from data: A simple cross-validation perspective, part vi: Hamiltonian systems .
- [49] Yoo, G.R., Owhadi, H., 2021. Deep regularization and direct training of the inner layers of Neural Networks with Kernel Flows. *Physica D: Nonlinear Phenomena* 426, 132952. doi:[10/gnrnn5](https://doi.org/10/gnrnn5).